

Yu. A. Kuzma-Kichta, A. S. Komendantov,  
Yu. G. Khasanov, and M. N. Burdunin

UDC 536.248.2.001.05

Data have been obtained on the bounds to the transitional region and the maximal wall temperature fluctuations in a heat-transfer crisis.

When a two-phase flow moves in a heated tube, there are fluctuations in wall temperature  $T_w'$ , which vary along the tube and are dependent on the working parameters; substantial fluctuations over a fairly extended region, the transitional one, accompany the heat-transfer crisis. Those fluctuations together with corrosive effects may cause premature failure. Information on these pulsations is necessary to construct sound models. Some data have been given [1-5] on these fluctuations on crisis onset, but they are mainly qualitative, as the fluctuations were measured with antiquated apparatus. Not much is known about how the transition-region characteristics are dependent on the working parameters.

We have made measurements with a rising water flow in a tube and a channel having complicated geometry with the apparatus described in detail in [6]; the Kh18N10T steel tube was 2 m long, internal diameter 8 mm, and wall thickness 1 mm. The channel had a 0.5 mm wall and represented the section of a cell formed by four adjacent tubes 13 mm in diameter placed with a pitch of 15 mm ( $d_{eq} = 5.6$  mm). The working parts were heated directly with line-frequency current. Chromel-alumel thermocouples were welded directly to the outer surfaces, wire diameter 0.2 mm, minimum couple pitch 25 mm.

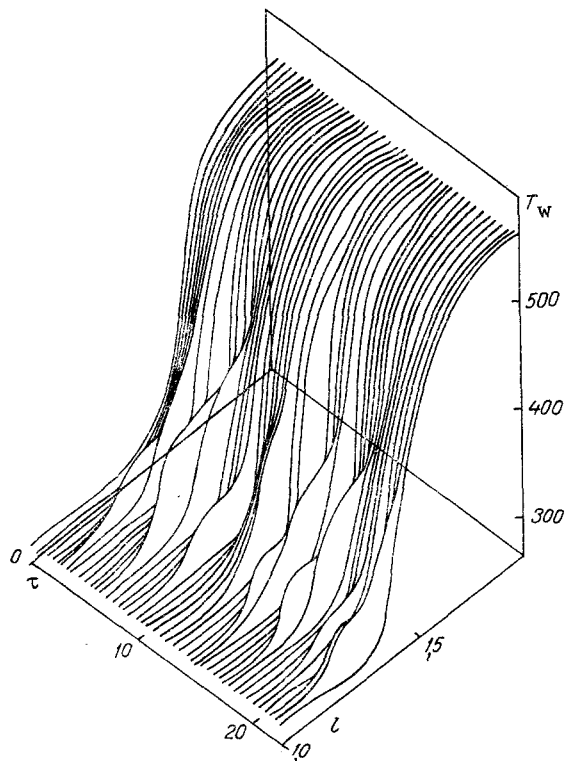


Fig. 1. Channel wall temperature as a function of time at 6.59 MPa,  $\rho W = 157$  kg/m<sup>2</sup>·sec,  $q_w = 229$  kW/m<sup>2</sup>, and  $x_{in} = -0.03$ ;  $T_w$  in °C,  $l$  in m, and  $\tau$  in sec.

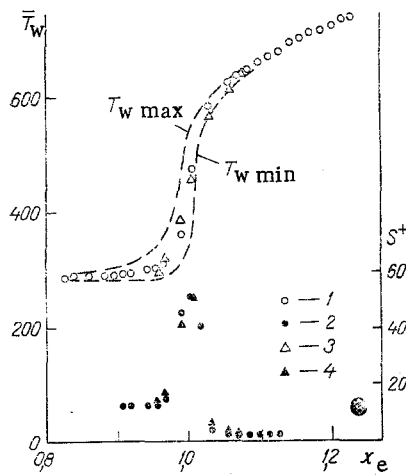


Fig. 2

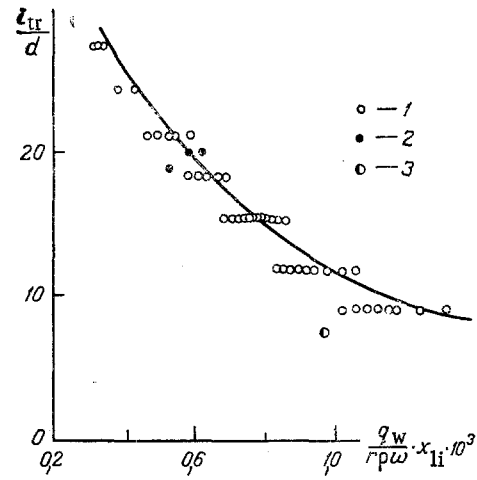


Fig. 3

Fig. 2. Variations in wall-temperature fluctuations (2 and 4) and wall temperature (1 and 3) along sections: 1 and 2) from 10 measurements; 3 and 4) data from prolonged interrogation,  $S^+$  in  $^{\circ}\text{C}$ .

Fig. 3. Transition-region lengths: 1) our results; 2) [5]; 3) [9].

We recorded the wall temperatures and the working parameters; the system provided digital recording with a computerized suite and continuous wall temperature recording. In the second case,  $T_w$  was measured with a four-channel amplifier having DC decoupling. The amplified signal went to a multichannel tape recorder and was processed by the computer. The analog signal was used in determining the necessary sensor interrogation times and frequencies, the intervals being 160 sec and four measurements a second correspondingly. Each experiment involved two stages. In the first, all the sensors were interrogated on 10 cycles. Each cycle lasted about 5 sec. The second involved prolonged interrogation, including for the thermocouples on the wall in the transition region. After the measurements, there were calculations on the means and standard deviations. The data were output to a printer as tables and graphs and were written to magnetic tape. Figure 1 shows the  $T_w$  pattern along the channel for various instants separated by about 0.5 sec; there are evidently complicated processes in the transition region. The fluctuations  $T_w'$  initially increase but decrease towards the end of the transition region. The time intervals corresponding to liquid contact are at first substantial but then decrease and become zero in the transcritical region. Figure 2 shows how the equilibrium steam content  $x_e$  influences the averaged wall temperature  $\bar{T}_w$  and the standard deviations in the fluctuations  $S^+$  (the dashed lines are the maximal and minimal  $T_w$  in the transition region) at 5.6 MPa,  $\rho_w = 205 \text{ kg/m}^2 \cdot \text{sec}$ ,  $q_w = 370 \text{ kW/m}^2$ , and  $x_{in} = 0.23$ . Here and subsequently,  $q_w$  is the heat flux density at the wall corresponding to the crisis onset. The  $\bar{T}_w$  and  $S^+$  curves in the two stages virtually coincide, so the transition-region bounds can be defined reliably from 10 measurements in accordance with the [7] method.

We recorded  $T_w$  fluctuations in the transition range for  $P = 0.55\text{--}7.20 \text{ MPa}$ ,  $\rho_w = 100\text{--}603 \text{ kg/m}^2 \cdot \text{sec}$ ,  $q_w = 100\text{--}1000 \text{ kW/m}^2$ , and steam contents  $x_{in} = -0.28$  to 0.66. The start of the transition region corresponds to the limiting steam content  $x_{li}$ , for which a relationship exists [8] for circular tubes:

$$x_{li} = 1 - 64,3 \left[ \frac{q_w}{r \sqrt{\rho''^4} \sqrt{\sigma g (\rho' - \rho'')}} \right]^{0,28} \left[ \frac{\rho_w v'}{\sigma} \sqrt{\frac{\rho'}{\rho''}} \right]^{1,25} \quad (1)$$

Somewhat lower  $x_{li}$  apply for the complicated channel, because of the geometry; the transition-region length  $l_{tr}$  is mainly dependent on  $q_w/(r\rho\omega)$  and  $x_{li}$ . Figure 3 shows  $l_{tr}$  data derived in the above ranges, which may be described with  $\pm 20\%$  deviations by

$$\frac{l_{tr}}{d} = 7,5 + 30e^n, \quad (2)$$

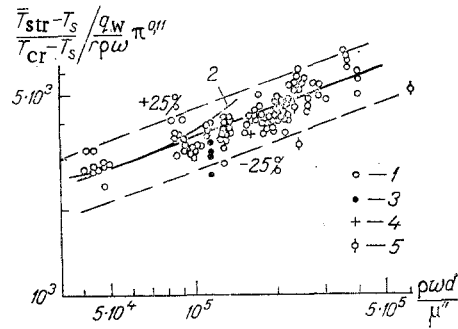


Fig. 4. Wall temperatures at the start of the transcritical region: 1) our results; 2) calculation from [7]; 3) [5], water; 4) [9], water; 5) [10], freon-22.

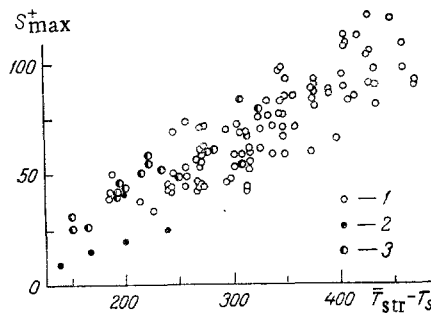


Fig. 5. Wall-temperature fluctuations in the transition region: 1) our results; 2) [5]; 3) [7].  $S_{max}^+$ ;  $T_{str} - T_s$ , °C.

in which

$$n = -6,3 \cdot 10^4 \left( \frac{q_w}{r \rho \omega} x_{II} \right)^{1,5}.$$

This formula also described the  $\ell_{tr}$  derived by our method from the [5, 9] data; when underheated liquid is supplied, it is necessary to raise  $q_w$  substantially in order to obtain a transcritical region, and in that case,  $\ell_{tr}$  is reduced to a value comparable with the thermocouple pitch. As it is necessary to measure  $T_w'$  in not less than three sections to estimate  $\ell_{tr}$ , the minimal  $\ell_{tr}$  recorded here was 50 mm.

The wall temperature corresponding to the end of the transition range, where there is a lower level in  $T_w'$ , is called the temperature for the start of the transcritical region  $\bar{T}_{str}$ ; the data have been fitted (Fig. 4) to the following relationship for the above parameter range with a  $\pm 25\%$  error:

$$\frac{\bar{T}_{str} - T_s}{T_{cr} - T_s} = 62,8 \frac{q_w}{r \rho \omega} \left( \frac{P}{P_{cr}} \right)^{0,11} \left( \frac{\rho \omega d}{\mu''} \right)^{0,35}. \quad (3)$$

Figure 4 also shows results for water with complicated geometry [7], circular tubes [5, 9], and results for freon-22 [10]. There is satisfactory agreement.

The strength characteristics are substantially dependent on  $T_w'$ ; Fig. 5 shows  $S_{max}^+$  in the transition region as a function of the temperature difference  $\Delta T_{str} = \bar{T}_{str} - T_s$ . The two increase together and the first corresponds to about a quarter of the second.

These results have been obtained on measuring  $T_w$  at the outer surface, but it has been shown [11] that the reduction in amplitude or change in frequency for  $T_w'$  for a wall thickness of 1 mm will be slight.

These data can be used in devising heat-transfer crisis models and in analyzing reliability for steam-generating equipment.

#### NOTATION

$T'_w$ , wall temperature fluctuations;  $d_{eq}$ , equivalent diameter;  $x_e$ , equilibrium mass steam content;  $\bar{T}_w$ , time-averaged wall temperature;  $S^+$ , standard deviation in wall temperature fluctuations;  $P$ , pressure;  $\rho W$ , mass velocity;  $q_w$ , wall heat flux density corresponding to crisis onset;  $x_{in}$ , steam content at inlet;  $r$ , latent heat of evaporation;  $\sigma$ , surface tension;  $g$ , acceleration due to gravity;  $\rho'$ , liquid density on saturation line;  $\nu'$ , kinematic viscosity of water on saturation line;  $x_{li}$ , limiting steam content;  $l_{tr}$ , transition-region length;  $d$ , diameter;  $\bar{T}_{str}$ , time-averaged temperature for start of transcritical region;  $T_g$ , saturation temperature;  $T_{cr}$ , critical temperature;  $P_{cr}$ , critical pressure;  $\mu''$ , dynamic viscosity of steam on saturation line;  $S_{max}^+$ , maximal standard deviations in wall temperature fluctuations;  $\tau$ , time;  $l$ , length;  $\pi = P/P_{cr}$ , reduced pressure.

#### LITERATURE CITED

1. I. S. Kudryavtsev, B. M. Lekakh, B. L. Paskar', et al., *Teploénergetika*, No. 11, 63-65 (1986).
2. P. L. Kirillov, N. M. Turchin, N. S. Grachev, et al., *At. Énerg.*, 54, No. 5, 330-333 (1983).
3. Yu. V. Krasnoukhov, N. S. Kudryavtsev, B. L. Paskar', et al., *Improving Heat-Transfer Performance in Power Equipment* [in Russian], Leningrad (1981), pp. 86-96.
4. B. V. Kebabze, *At. Énerg.*, 39, No. 4, 250-254 (1975).
5. S. Nakanishi, S. Yamauchi, S. Ishigai, et al., *Seventh International Heat Transfer Conference*, Vol. 4, Munich (1982), pp. 315-320.
6. M. N. Burdunin, Yu. A. Zvonarev, A. S. Komendantov, and Yu. A. Kuzma-Kichta, *Heat and Mass Transfer VII: Proceedings of the Seventh All-Union Conference of Heat and Mass Transfer*, Vol. 4, Section 2 [in Russian], Minsk (1984), pp. 41-47.
7. A. S. Komendantov, Yu. A. Kuzma-Kichta, and M. N. Burdunin, *Teploénergetika*, No. 1, 64-66 (1987).
8. Yu. G. Khasanov, A. S. Komendantov, Yu. A. Kuzma-Kichta, and M. N. Burdunin, *Teploénergetika*, No. 7, 69-71 (1987).
9. O. K. Smirnov, V. I. Lezin, L. G. Pashkov, et al., *Trudy MÉI*, Issue 200, 22-37 (1974).
10. K. Nishikama, S. Yoshida, H. Mori, and H. Takamatsu, *Int. J. Heat Mass transfer*, 29, No. 8, 1245-1251 (1986).
11. V. A. Vorob'ev, P. L. Kirillov, O. V. Remizov, and V. I. Subbotin, *Heat and Mass Transfer*, Vol. 2, Part 1 [in Russian], Minsk (1972), pp. 67-78.